Physica A 392 (2013) 4701–4716

Contents lists available at SciVerse ScienceDirect

Physica A

journal homepage: www.elsevier.com/locate/physa

Dynamics of the HIV infection under antiretroviral therapy: A cellular automata approach

Ramón E.R. González [a,1], Sérgio Coutinho [a], Rita Maria Zorzenon dos Santos [a,*], Pedro Hugo de Figueirêdo [b]

[a] *Laboratório de Física Teórica e Computacional, Departamento de Física, Universidade Federal de Pernambuco, 50670-901, Recife, Pernambuco, Brazil*

[b] *Departamento de Física, Universidade Federal Rural de Pernambuco, 52171-900, Recife, Pernambuco, Brazil*

HIGHLIGHTS

- We include drug therapies on a cellular automata model that describes the dynamics of HIV infection.
- The effectiveness of different drug types depends on the infection load at each time step.
- The model reproduces the time scales in which relevant changes on T cell counts occur during the drug therapy.
- The model reproduces qualitatively the results observed for the first two years of treatment on different cohort studies.

ARTICLE INFO

Article history:
Available online 7 June 2013

Keywords:
Cellular automata
HIV infection
Pattern formation
Population dynamics
Drug therapies

ABSTRACT

The dynamics of human immunodeficiency virus infection under antiretroviral therapy is investigated using a cellular automata model where the effectiveness of each drug is self-adjusted by the concentration of $CD4^+$ T infected cells present at each time step. The effectiveness of the drugs and the infected cell concentration at the beginning of treatment are the control parameters of the cell population's dynamics during therapy. The model allows describing processes of mono and combined therapies. The dynamics that emerges from this model when considering combined antiretroviral therapies reproduces with fair qualitative agreement the phases and different time scales of the process. As observed in clinical data, the results reproduce the significant decrease in the population of infected cells and a concomitant increase of the population of healthy cells in a short timescale (weeks) after the initiation of treatment. Over long time scales, early treatment with potent drugs may lead to undetectable levels of infection. For late treatment or treatments starting with a low density of $CD4^+$ T healthy cells it was observed that the treatment may lead to a steady state in which the T cell counts are above the threshold associated with the onset of AIDS. The results obtained are validated through comparison to available clinical trial data.

1. Introduction

The dynamics of human immunodeficiency virus (HIV) infection has challenged researchers in various fields of knowledge due to its extremely complex pathogenesis and the extent of medical and social impact that its understanding should provide. The HIV pandemic remains a major global public health challenge: more than 60 million people have been infected

* Corresponding author. Tel.: +55 81 99629963; fax: +55 81 21268450.
E-mail addresses: zorzenon@df.ufpe.br, rita.zorzenon@gmail.com (R.M. Zorzenon dos Santos).
1 Permanent address: Departamento de Física, Universidade Federal Rural de Pernambuco, 52171-900, Recife, Pernambuco, Brazil.

0378-4371/$ – see front matter © 2013 Elsevier B.V. All rights reserved.
http://dx.doi.org/10.1016/j.physa.2013.05.056

with the HIV virus and nearly 30 million people have died of AIDS, since its beginning. Recent data reveals that in 2010 there were an estimated 34 million people living with HIV, 2.7 million newly infected, and 1.8 million AIDS-related deaths [1]. This latter annual indicator is steadily decreasing since 2004 due to different factors including among them the increasing availability of antiretroviral therapy. In particular regions, such as in North America and Western and Central Europe, deaths due to AIDS began to decline soon after antiretroviral therapy was introduced in 1996 [1].

Currently joint multidisciplinary efforts are focused towards two highly related goals: the desperate search for developing a prophylactic vaccine and the achievement of therapies that provide long-term drug-free remissions in HIV-infected patients [2–4]. In particular, mathematicians, bio-mathematicians and physicists have invested great efforts in this subject through the formulation of mathematical models to describe the time evolution of the virus population and the repertoire of cells involved in the infection.

In the nineties, after the appearance of antiretroviral therapies, a large number of mathematical models have been formulated to describe HIV infection and its interaction with the immune system, manifested mainly by the observed decrease of $CD4^+$ T cell population. Most of these models were composed of a system of ordinary differential equations (ODEs) describing the time evolution of the average populations of involved cells and viruses considered in each model. Both deterministic and stochastic models were considered. Among them, for instance, the earlier works of Perelson et al. [5,6], and that of Kirschner and Webb [7] and Wei et al. [8], who investigated strategies in the mono-therapy in the presence of drug resistant strains. For an intuitive introduction on the basic elements and concepts involved in modeling the dynamics of HIV and other viruses and their interactions with the immune system, the text by Nowak and May [9] is highly indicated, while the one of Perelson and Nelson [10] is recommended for a review of mathematical models formulated at the time.

Over the past decade, with the development of potent antiretroviral therapies, based on a combination of three or more drugs the models become more complex and sophisticated. These models include new types of cells that participate in the immune response (e.g. Refs. [11–13]) and consider their interactions with free virions and with the reverse transcriptase and protease inhibiting drugs [14]. Other aspects involved in antiretroviral therapies, such as drug resistant strains, different protocol strategies and adherence to drug treatments, were also investigated using models based on ODEs [15,16].

The models based on systems of ordinary differential equations (ODE) contributed significantly to the understanding of various aspects of the dynamics of HIV infection. However, in general, such compartmentalized models describe the time average behavior of virus and cell populations but they cannot capture the properties of the dynamics of HIV infection emerging from local interactions among such populations.

Cellular automata are an alternative and powerful methodology to the study of spatiotemporal systems where complex phenomena emerge from many simple local interactions. In particular, CA models have shown to be appropriated to describe for instance the common HIV infection pattern observed in patients [17] using a unique set of parameters. This approach, although less explored, has been used since the beginning of the 90s to describe some aspects of HIV infection [18–20].

The model we study in this work is an extended version of a previous CA model, from now on referred to as HIV-CA, proposed by two of us in 2001 to describe the course of HIV infection. Through the behavior of the population of T cells in lymph nodes [17] the HIV-CA model shows that the combination of a healthy immune system with high viral proliferation and mutation rates and a fair amount of spatial localization of the target cells in lymphatic tissues [21] describes the entire course of infection. The local interactions occurring between cells and virus in the lymph nodes allow for reproducing qualitatively the three stages (primary infection, clinical latency and onset of AIDS) and the two time scales involved on the HIV dynamics. The results have been proved to be robust on different regions of the parameter space [22,23] contrary to what was claimed in Ref. [24]. A rigorous mathematical analysis of the time scales and dynamical aspects of the HIV-CA model was carried out by Burkhead et al. [25] using ergodic theory and techniques like topological dynamics. Inspired by these results other extended versions of the HIV-CA model have been proposed to investigate other aspects of HIV infection and antiretroviral drug therapies [26–30].

The aim of this work is to investigate the dynamics of $CD4^+$ T cells during HIV infection under the action of multiple antiretroviral therapy introducing an extended version of the HIV-CA model [17] that include some of the mechanisms of antiretroviral therapies currently in use.

In the following Sections 1.1 and 1.2 we briefly describe the pathogenesis of HIV and discuss the mechanisms in which the antiretroviral therapies are based. This will help the reader to better understand the extended HIV-CA model proposed in this work.

1.1. The HIV pathogenesis

The HIV infection occurs when viral particles of HIV are transferred from one individual to another by sexual or parenteral routes. After binding to the target cells the viral particle is transported to lymph nodes where its replication takes place establishing a permanent infection [31]. The main target of HIV are cells of the immune system such as T cells, macrophages and dendritic cells and the viral entrance depend on CD4 receptors and co-receptors CCR5 (macrophages, dendritic and T cells) or CXCR4 (only T cells).

After binding to the appropriate receptors, the HIV enters the cell by endocytose and fusion [32] and release of the HIV viral core into the cell interior. Successful uncoating generates the viral reverse transcription and its completion gives rise to a viral double stranded cDNA that may have different fates. From the point of view of virus replication the most important fate is its effective integration into the host chromosome [33]. The HIV provirus can integrate in many different

chromosome locations and most infected cells harbor more than one provirus. The chromosome environment helps the provirus transcriptional activity or favor quiescence. After successful transcription of viral genome, a dozen of transcripts are generated and transported from the nucleus to the cell cytoplasm. Specific viral proteins (enzymatic and structural) are produced and transported to plasma membrane where the viral assembly is facilitated giving rise to new progeny virions that would be released by the infected cell [34]. The HIV high mutation rate allows for refinement and optimization of its interactions with the host proteins promoting its fast replication and spreading. The silent provirus reservoir (resulting from quiescent states) is responsible for the non-complete eradication of HIV infection after potent antiviral therapies and allows for the reemergence of HIV burden when the immune defenses grow weaker.

The successful cell infection process leads to its death after the viral replication cycle is complete. The low levels of $CD4^+$ T cells observed in infected patients therefore can be explained, among other mechanisms, by the viral cycle itself and by the increasing rates of apoptosis generated by immune system cytotoxic mechanisms. When $CD4^+$ T cell counts decrease below a critical threshold, the cell-mediated immunity is compromised leading the infected individual to *acquire immunodeficiency syndrome* (AIDS). At this stage the individual becomes progressively more susceptible to AIDS and non-Aids opportunistic infections increasing the individual's probability of dying from complication of one of them [31].

The typical course of HIV infection observed in non-treated patients is expressed by the time evolution of $CD4^+$ T cell counts and plasma viremia titer, as illustrated in Fig. 1 of Ref. [35]. The HIV infectious process in non-treated patients exhibits a common pattern with three distinct phases and two time scales that may vary from patient to patient [35,36]:

Primary infection: it is the first stage of the disease characterized by a broad viral dissemination, which declines markedly in weeks after the emergence of the HIV-specific immune response [37]; its duration is delimited by the decrease of the viral burden to (almost) undetectable levels without its complete elimination.

Clinical latency period: it is the period of time that follows the primary infection and may vary from weeks (fast progression disease) to years (10 years or more for non-treated patients); during this stage patients are usually asymptomatic but in all cases a gradual but progressive decrease on $CD4^+$ T cell counts in the presence of a very low viral burden is observed [35].

Onset of AIDS: when the concentration of the T cells becomes lower than a threshold value, which can vary between 350 and 200 cells/mm^3, the patient is considered to have acquired the immunodeficiency syndrome and to be at the risk of opportunistic diseases [38]. From now on we shall refer to this critical $CD4^+$ T cell count as the AIDS threshold.

The HIV infection is a multifactorial disease and the progressive depletion of $CD4^+$ T cells is one of its clinical hallmarks. Studies of infected individuals' lymphoid tissues have shown that these tissues become HIV reservoirs and generate the necessary environment for viral replication [39]. The ability to measure the plasma viremia allowed for many insights about the HIV pathogenesis, including the understanding of the importance of the balance between virus productions and T cell dynamics [40]. It also made it possible to use the viral load of untreated patients as a prognosis for disease progression. In the past decades, among many advances and discoveries related to HIV infection, we have witnessed an enormous development of more effective antiviral drugs improving the quality of and lifetime of infected individuals. However, the understanding of what would generate HIV immune protection remains an open question and a challenge.

1.2. Antiretroviral therapies

The spectrum of HIV antiviral drugs developed up to now is mainly focused on the vulnerable points of the virus replication cycle. The first effective drug against HIV that appeared in the late 80's was the reverse transcriptase inhibitor [41,42] that inhibits viral replication and since then different types of this enzyme have been used in HIV drug therapies. The isolation of HIV protease enzyme has facilitated the design of protease inhibitors, another class of antiretroviral drugs (ARV) that also interferes with the HIV replication. Later on fusion inhibitors appeared blocking the fusion of the viral envelope and the entrance of the virus into the cell membrane and integrase inhibitors impeaching the insertion of the proviral DNA to host cell chromosomes. Up to now the US Food and Drugs Administration (FDA, USA) has approved more than 35 ARV drugs and therapies that have had a great impact on the control viral replication [31,43]. The use of drug therapies for more than two decades [42] has changed the pattern of morbidity and mortality associated with HIV infection [44] in nations where such drugs are available for infected patients.

In general antiretroviral therapies (ART) involve the use of two or more classes of antiretroviral drugs. The most common combinations usually consist of two nucleoside *reverse transcriptase inhibitors* (NRTI) plus either a protease inhibitor (PI) or a non-nucleoside reverse transcriptase inhibitor (NNRTI). The *nucleoside/nucleotide* reverse transcriptase inhibitors (NRTI), and the *non-nucleoside* reverse transcriptase inhibitor (NNRTI) are classified as competitive substrate inhibitors and act in very similar ways: when one of them is incorporated into the growing viral DNA chain, its synthesis is halted, inhibiting HIV replication [41,42]. *Protease inhibitors* (PI) play an essential role in viral reproduction. This enzyme is fundamental for the formation of the HIV protein coat and its blockage leads to the production of non-infectious virus species [45,46]. Currently, there are nine PIs approved for clinical use but resistance to all protease inhibitors has been observed and the genetic basis of resistance has been well documented over the past 15 years.

Although the current adopted therapies may improve the lifetime of individuals, they are toxic, have side effects [42] and do not cure the individual. When the treatment is effective, the important consequence is a decrease in the viral load (that

can reach up to 90%) after few weeks when compared to the initial baseline at the time of treatment's initiation. After six months, these values may fall to undetectable levels for common tests.

In this work, the inhibitory effects of ARV drugs would be incorporated into the rules of the HIV-CA model, taking into account its intrinsic effectiveness as explained in the next section.

The paper is organized as follows: in Section 2 we briefly review the rules of HIV-CA model and present its extended version including ARV drug effects on the HIV dynamics that will be the subject of study in this paper. In Section 3, the results of the model are presented and discussed, and also compared with clinical data available in literature. Finally, in Section 4 the conclusions are summarized.

2. Cellular automata model for HIV infection under antiretroviral therapies

A major challenge on modeling the dynamics of the HIV infection is to capture the mechanisms that allow for the persistence of the viral infection even in the presence of the immune response. The viral persistence is the main feature that makes the HIV infection different from other viruses. This point was well described in the HIV-CA model and therefore we expect that by extending the model to include some of the effects of drug therapies we would also learn more about the drug effects and maybe gain insights on the subject.

Previous studies using models based on the HIV-CA model were proposed aiming to include the mechanisms of antiretroviral therapies. We highlight the works by Sloot et al. [26] and Shi et al. [29], which consider mechanisms to describe the effectiveness of treatments as we also do here. On the model presented in Ref. [26] the effects of the drug therapies are described by a parameter that reduces the extent of the infected cell's action on its neighborhood. Besides, they consider a time dependent decreasing linear probability function to simulate the decrease of the effectiveness of the drugs used in the treatment. With such *ad hoc* mechanisms their results indicate the possibility of survival of individuals, depending on the effectiveness of drugs and of certain response functions. Their results also suggest that the high quality of medicines can prevent, in a way, replication of the virus and the emergence of resistant strains. In Ref. [29] a similar mechanism based on the viral load was considered to self-adjust the active neighborhood of an infected cell; in addition a drug resistance mechanism was introduced through an exponential decay function without any biological justification. Shi et al. [29] also include in their model a new pool of the $CD4^+$ T cells, which are recruited from regular healthy cells, representing the cells that have been exposed to HIV but remain healthy as a consequence of the treatment. Their results reproduce the three stages of the HIV dynamics and suggest the possibility to adopt a new type of controlled therapy by adjusting drug doses and its schedule. However, no validation by comparison with clinical data or analysis of the parameter space is provided.

It is important to notice that none of the above mentioned works [26,29] considered the effectiveness of treatment as a direct function of the infection level at each instant of time as suggested by the medical and biological reality [6,47,48]. The model introduced in the present work consider mechanisms of antiretroviral therapies whose effectiveness that would be self-adjusted at each time step according to the infection intensity, in this case represented by the density of infected $CD4^+$ T cells.

2.1. Present model

The cellular automata model considered in this work extends the HIV-CA model, previously proposed in Ref. [17] by including new rules and new cell states that allow for considering the effects of ARV therapies on the dynamics of the HIV infection. In the model we will consider that the therapy would start at time t_0 corresponding to any time of the regular dynamics of infection in the absence of treatment. Therefore the dynamics preceding the initiation of drug therapy is the same one defined on the HIV-CA model which is briefly reviewed below.

HIV-CA model

This model describes the dynamics of HIV infection in lymphoid tissue by considering the interaction among the immune cells and HIV [17]. In the model the cells are described by four-state automata representing different states of the $CD4^+$ cells during the course of infection: susceptible healthy cells H, productive infected cells A_1 not yet identified by the immune system, less productive infected cells A_2 already detected by the immune system but still capable of infecting healthy cells and D dead cells that give place to vacancies in the spatial structured model. A square lattice, each site being occupied by a target cell, simulates the lymphoid tissues. In the initial configuration the great majority of the sites are occupied by healthy cells but a small concentration p_{HIV} of infected cells (A) is considered. At each time step we perform a parallel updating using periodic boundary conditions and following the chart flow presented in Fig. 1 that describes the following rules:

Rule 1: A healthy cell H becomes an infected-A_1 cell, if it has at least one infected-A_1 cell among its nearest neighbors, or at least four ($R = 4$) neighboring cells in the state infected-A_2. Otherwise, it remains healthy H.

Rule 2: An A_1-infected cell remains τ time steps in this state, after which it becomes an infected-A_2 cell. τ represents the period of time necessary for a new infected cell that carries new viral particles to be detected by the immune system.

Rule 3: An A_2-infected cell becomes a dead cell (vacancy) (D-cell) in the next time step.

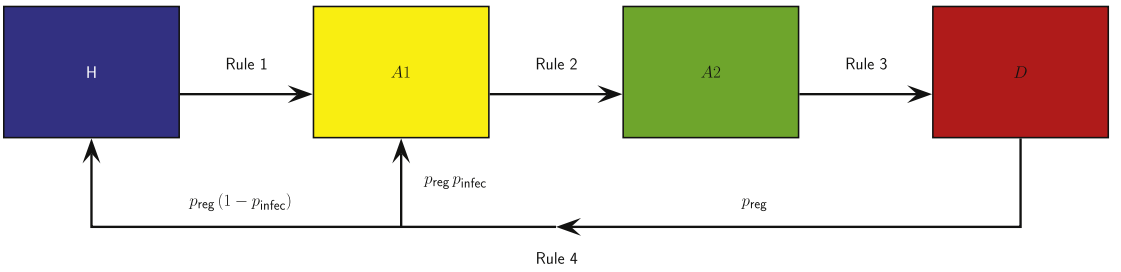

Fig. 1. Flow chart of the progression of the HIV-CA model (Ref. [17]), which describes the present model before initiation of treatment.

Rule 4: A dead cell D (vacancy) is replaced by a healthy cell H with probability $(1-p_{\mathrm{infec}})\,p_{\mathrm{reg}}$, or by an A_1-infected cell with probability $p_{\mathrm{reg}}\,p_{\mathrm{infec}}$, otherwise it remains in a dead state. The replacement simulates the dynamics generated in lymphoid tissues due to the blood incoming flux.

The rules and the model parameters were defined based on biological grounds and its values chosen consistently with clinical and experimental observations, as described in detail in Refs. [17,22,23].

Rules 1 and 2 mimic the spread of HIV infection by contact or proximity. Productive infected cells spread the virus to healthy neighboring cells either by direct contact or by release of viral particles in their neighborhoods. The difference between the two rules is related to the power of infection of the infected cells: infected cells not detected by the immune systems spread the infection more easily than those already detected. As shown before [23] τ is a key parameter for obtaining different time scales on the dynamics of the model since it regulates the time scale of primary infection. As we will show later on τ also defines the short-range time scale for the response to antiretroviral drugs treatment. Rule 3 mimics the depletion of the infected cells by the immune response. Rule 4 describes the replacement of dead cells by new $CD4^+$ T cells taking into account the hypothesis that the capacity of replenishment of the immune system is unaffected by infection, but also taking into account the fact that the vacancies can be occupied by infected cells coming from other compartments. Hence the probabilities p_{reg} and p_{infec} introduced in Rule 4 account for all mechanisms governing the (re) infection process [2,49–51].

Under treatment

In order to consider the effects and effectiveness of ARV therapies it is necessary to introduce three new states for healthy cells that would be considered after the beginning of the treatment ($t \geq t_0$). Specifically, these states would describe healthy $CD4^+$ T cells, which have absorbed either the reverse transcriptase inhibitor ($\mathrm{H_{RT}}$) or the protease inhibitor ($\mathrm{H_P}$) at any time, or simultaneously absorbed both inhibitors ($\mathrm{H_{RTP}}$). These states were originally conceived by Smith and Wahl [14] to describe the dynamics of $CD4^+$ T cells interacting with free virions and under the effects of reverse transcriptase and protease drug inhibitors in a model based on coupled ordinary differential equations. The need to consider the evolution of such states to $CD4^+$ T cells at each time step of the dynamics is justified by the fact that the average intracellular half-time of the inhibitors drugs is of the order of hours while the lifetime of an uninfected $CD4^+$ T cell is of the order of days.

When the treatment starts the rule concerning healthy cells should be split in new rules to account for the interactions of healthy cells and the drugs adopted in the therapy.

Healthy cells under therapy should continue to interact with viral particles (according to HIV-CA rules) but forcibly should also interact with drugs, which in the case considered here would possibly inhibit reverse transcriptase and/or protease. Any combination of these three possible interactions may occur at each step of the simulation. If a given healthy cell becomes infected and it has absorbed either or both drugs, it will produce a non-infectious virus. Therefore under treatment the new Rule 1 is summarized in Figs. 2 and 3(a) and explained as follows:

Rule 1a. Under treatment a healthy cell H state becomes $\mathrm{H_{RTP}}$ with probability $p_{\mathrm{RTI}} \times p_{\mathrm{PI}}$; or becomes $\mathrm{H_P}$ with probability $(1-p_{\mathrm{RTI}}) \times p_{\mathrm{PI}}$; or becomes $\mathrm{H_{RT}}$ with probability $p_{\mathrm{RTI}} \times (1-p_{\mathrm{PI}})$; or becomes an infected-$\mathrm{A_1}$ cell with probability $(1-p_{\mathrm{RTI}}) \times (1-p_{\mathrm{PI}})$ provided it has at least one infected-$\mathrm{A_1}$ cell or $R = 4$ $\mathrm{A_2}$ cells amongst its nearest neighbors, otherwise remains healthy H.

Rule 1b. A healthy cell $\mathrm{H_{RT}}$ becomes a $\mathrm{H_{RTP}}$ cell with probability p_{PI}; or remains a $\mathrm{H_{RT}}$ cell with probability $(1-p_{\mathrm{PI}}) \times p_{\mathrm{RTI}}$; or becomes an infected-$\mathrm{A_1}$ cell with probability $(1-p_{\mathrm{PI}}) \times (1-p_{\mathrm{RTI}})$ and if it has at least one infected-$\mathrm{A_1}$ cell or $R = 4$ $\mathrm{A_2}$ cells amongst its nearest neighbors, otherwise remains a healthy H cell.

Rule 1c. A healthy cell $\mathrm{H_P}$ becomes a $\mathrm{H_{RTP}}$ cell with probability p_{RTI}, or remains a $\mathrm{H_P}$ cell with probability $(1-p_{\mathrm{RTI}}) \times p_{\mathrm{PI}}$ or an infected-$\mathrm{A_1}$ cell with probability $(1-p_{\mathrm{PI}}) \times (1-p_{\mathrm{RTI}})$ and if it has at least one infected-$\mathrm{A_1}$ cell amongst its nearest neighbors, or at least $R = 4$ neighbors in infected-$\mathrm{A_2}$ state, otherwise remains a healthy H cell.

Rule 1d. A healthy cell $\mathrm{H_{RTP}}$ becomes a healthy cell H in the next time step.

It is important to note that a healthy cell H that absorbs one of two inhibitor drugs (or both) and has contact with an infected cell or viral particle will become infected but will no longer act as a productive infected-$\mathrm{A_1}$ cell, at most it will produce non-infective virus particles. Therefore, in case a healthy cell escapes from the inhibitory drug effects, it may become an infected-$\mathrm{A_1}$ cell capable of spreading the infection, as clearly illustrated in the flowcharts shown in Figs. 2 and 3(a).

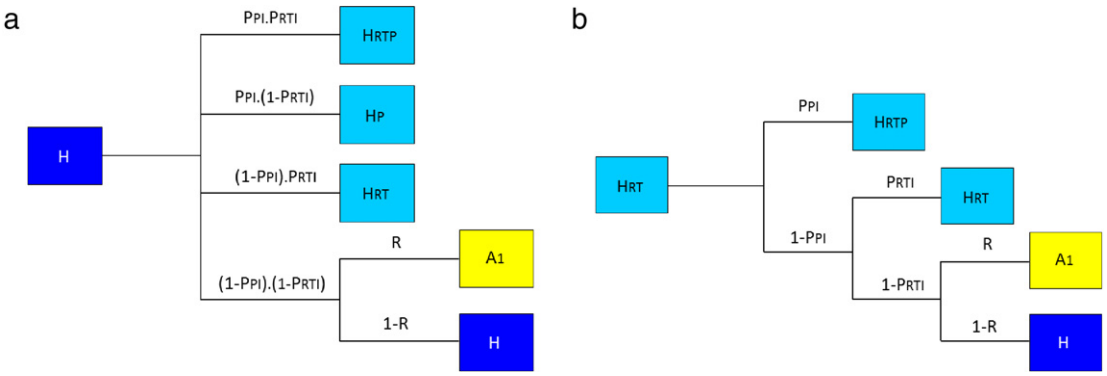

Fig. 2. Flowcharts of the progression of healthy $CD4^+$ T cells (panel (a)) and healthy-H_{RT} (panel (b)) under cART. Rectangles indicate the reservoirs of CA states of the cells: blue for the healthy H-cells, cyan for healthy cells that have absorbed inhibiting drugs (H_{RT}, H_P and H_{RTP}) and yellow for the infected-A_1 cells. R (1-R) indicates the compliance (non-compliance) of the conditions for infection to occur by contiguity, according to Rule 1. (For interpretation of the references to colour in this figure legend, the reader is referred to the web version of this article.)

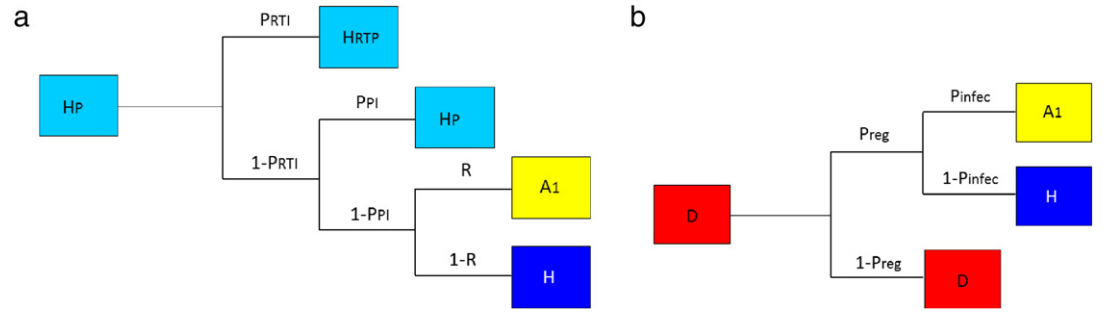

Fig. 3. Flowcharts of the progression of healthy-H_P cells (panel (a)) and dead-D cells (panel (b)) under cART. Rectangles indicate the reservoirs of CA states of the cells: blue for the healthy H-cells, cyan for healthy cells that have absorbed inhibitory drugs (H_{RT}, H_P and H_{RTP}), yellow for the infected-A_1 cells and red for dead D cells. R (1-R) indicates the compliance (non-compliance) of the conditions for infection to occur by contiguity, according to Rule 1. (For interpretation of the references to colour in this figure legend, the reader is referred to the web version of this article.)

Rule 1d describes the progression of healthy H_{RTP} cells, which had previously absorbed both RTI and PI drugs. Once the drug effects are ceased they become regular healthy H cells.

The eventual absorption of ARV drugs by infected-A_1 cells would not affect the dynamics of the model, since if it absorbs an RT inhibitor, its infective capacity will not change immediately, and before the inhibition effect takes place the cell may release its internal viral particles. On the other hand, if the PI inhibitor is absorbed, the viral protease is inhibited and new infectious virus particles cannot be released but the cell's infection capacity by direct contact still remains active. Therefore, in both cases, the cell would continue to act as a drug-free infected-A_1 cell and will evolves to the infected-A_2 state after τ time steps.

Finally, the replacement of dead cells follows the same rules defined on the HIV-CA model as described by the flow chart exhibited in Fig. 3(b).

Fig. 4 shows the closed flow chart (from now on referred as cART) of the states of automata after initiation of a combined ARV therapy where both kinds of drugs are considered.

Self-adjusting effectiveness

Many factors influence the effectiveness of antiretroviral treatments, which can vary widely among patients. The high rate of HIV replication and its inherent genetic variations are considered the chief hypotheses explaining the virus permanence. Mutations of the HIV genome confer resistance to drugs [45] suggesting that low levels of ongoing viral replication continue to persist as observed in patients that received cART for extended periods of time [52]. Pharmacokinetics and imperfect adherence to prescribed ARV drugs are other important factors for the failure of cART [53]. For instance, a high adhesion rate to treatment by HIV infected patients was observed to be associated with the increasing rates of viral suppression balanced by the increasing rates of drug resistance among patients [54].

However, since the current antiretroviral drugs are not able to eliminate all strains of virus, a significant population of virus-resistant infected cells remains active.

In the present study, the intracellular biochemical factors that influence the effectiveness, such as the susceptibility of inhibiting drugs is considered. The effects due to extracellular factors like pharmacokinetic and adherence will be taken into account later on.

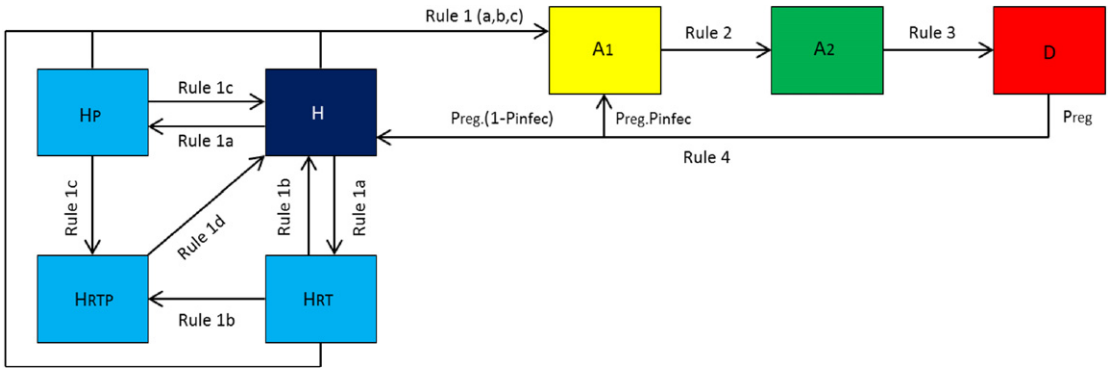

Fig. 4. Flow chart of the progression of the HIV-CA model including cART after initiation of therapy.

Recent studies show that after the initiation of antiretroviral therapy, there is a rapid decrease in HIV viral load in the first weeks (∼35 days) and a concomitant rise in the concentration of healthy CD4 cells [55,53]. However, since the current antiretroviral drugs are not able to eliminate all strains of virus the patient ends up developing a drug resistance, i.e., a population of cells remains infected by active resistant viruses. Thus, after initiation of therapy the drugs should become progressively less effective to the remaining population of infected cells. Following this reasoning, the reduction of the concentration of infected cells during the first weeks after initiation of treatment would also reflect the loss of effectiveness of drugs for this population.

Since the drug action has limited effects on disease control and development of new resistant strains of viruses, after a certain time after the initiation of the drug therapy the population of infected cells would reach a minimum value that would depend on the patient's conditions and on the adopted drug therapy. However, given that new drug resistant and non-resistant strains of virus continue to be released, the population of infected cells starts to grow again after reaching its minimum concentration. The balance between the growth of drug resistant and non-drug resistant virus populations (infected cells) and the self-adjusted drug effectiveness will lead to fluctuations in the population of infected cells till reaching a steady state.

Here we consider a self-adjusting mechanism of drug effectiveness that depends on the concentration of infected cells and follows some biological requirements: (a) the effectiveness should have a maximum value for the concentration of infected cells at time of treatment initiation; (b) just after the beginning of the treatment, such dependence should decrease the effectiveness to its smallest value when the concentration of infected cells has reached its minimum value; (c) it should reproduce the viral rebound (increase in viral turnover) observed experimentally [56] and the correlated increase of the population of infected cells leading to its stationary behavior. The self-adjusting mechanism would be defined independently for each type of drug, RT or P, and would be described by the probabilities p_{RTI} and p_{PI} on the rules of the model. Each probability would be a function of infected cell concentrations at time t satisfying the above requirements, and among many other possibilities it would be described by the following function:

$$p_j(t) = p_{0j}\left(\frac{D_I(t)}{D_{I0}}\right)^{\frac{2D_{I0}}{1-D_{I0}}}\left(\frac{1-D_I(t)}{1-D_{I0}}\right)^2 \tag{1}$$

where $p_j(t)$ is the effectiveness at instant t after initiation of treatment, the index $j = \mathrm{RTI}$ or PI denoting the RT and P inhibitors, respectively. p_{0j} is the maximum value of effectiveness, which characterizes the intrinsic effectiveness of the corresponding type of drug. D_{I0} corresponds to the concentration of infected cells at the initiation of treatment while $D_I(t)$ corresponds to this concentration at a subsequent time t. Fig. 5 exhibits plots describing the 90% drug effectiveness function for four different initial concentrations of infected cells. Each plot should be used to adjust the corresponding inhibiting drug probability (for mono or combined therapies) initiated with the corresponding D_{I0}. The red curve, for instance, describes the effectiveness dependence on the infected cell density for the particular case when $D_{I0} = 0.6$, which corresponds to the drug effectiveness of $p_{0j} = 90\%$. In other words, given D_{I0} at t_0 the drug effectiveness curve is defined with its maximum value p_{0j} at D_{I0}, while other values of $p_j(t)$ in the following time steps would be determined by the ordinate associated with the corresponding abscissa $D_I(t)$. In the example above, if the concentration of infected cells drops, the left hand side of the curve will describe the behavior of the effectiveness, while the right hand side would describe this behavior when this concentration eventually becomes greater than 0.6. By choosing this mechanism to describe the treatment's effectiveness we would be able to describe the particularities that can be observed for different patients (samples) using the same protocol.

3. Results

The CA simulations were performed on a two-dimensional lattice of size $L = 700$ using periodic boundary conditions and considering the *Moore neighborhood* for each cell. For comparison purposes we have adopted the same parameters used in the original model [17], which are $p_{\mathrm{HIV}} = 0.05$, $p_{\mathrm{infec}} = 0.00001$, $p_{\mathrm{reg}} = 0.99$ and $\tau = 4$.

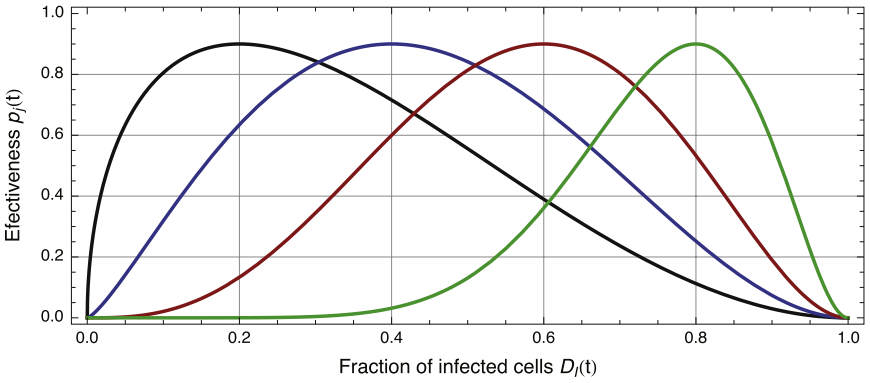

Fig. 5. Effectiveness $p_j(t)$ as a function of the concentration of infected cell $D_I(t)$ at the time t after initiation of treatment. For all plots the maximum value of effectiveness adopted is $p_{0j} = 0.9$ but each plot corresponds to a different density of infected cells at the time of initiation of treatment: $D_{I0} = 0.2$ (black), 0.4 (blue), 0.6 (red) and 0.8 (green), respectively. (For interpretation of the references to colour in this figure legend, the reader is referred to the web version of this article.)

We investigate the changes over the dynamics of infection produced by three types of antiretroviral therapy initiated from t_0 and maintained without interruptions. Two types of mono-therapies (RT or P inhibitors) and the combined therapy are considered by taking into account in each case *low*, *moderate* and *high* effectiveness. We analyze the results of the model (concentration of healthy, infected and dead cells) with respect to the drugs utilized in the different treatments. Initially, we discuss the changes over the infection dynamics in a long time scale (of the order of years) until the steady state is reached, focusing subsequently on the variations of such concentrations on a short time scale (of the order of weeks) after the beginning of treatment.

3.1. HIV infection under ARV therapy in long time scales

Fig. 6 shows the results obtained for mono (RTI and PI) and combined (cART) therapies starting at $t_0 = 300$ weeks for drugs of low ($p_{0j} = 0.5$) effectiveness. For the same initial set of parameters, the different concentrations of cells shown on panels (a) and (b) exhibit similar behaviors for the two types of mono-therapies, but differ substantially from the case *without* any treatment on panel (d). Besides the disturbance observed on the short time scale after the treatment's initiation, the major differences observed on the plots presented on panels (a) and (b) compared with those on panel (d) are the steady state cell concentrations: a reduction in infected and dead cell concentrations and a corresponding increase of the concentration of healthy cells, leading the system slightly above the threshold of AIDS (∼20%). When cART is considered, as shown on panel (c), such a difference with respect to panel (d) is magnified due to the combined action of two different types of drugs. The resulting effects seem to be cumulative driving the system above the threshold of AIDS (∼40%) although still keeping the healthy $CD4^+$ T cell concentration below the level of non-infected individuals.

The effects caused by the variation from low to moderate and high drug effectiveness are explored for the combined drug therapy, while maintaining the same initial conditions at the beginning of the treatment. Fig. 7 illustrates such a comparison. We observe that there is a decrease of the steady-state infected cell concentration (Fig. 7(a)) and an increase of the healthy cell one (Fig. 7(b)) when effectiveness is increased form 50% to 70% and 90%. Furthermore, the effects of drug therapies emerge on the same short time scale (a few weeks) regardless of its effectiveness, an aspect that will be discussed in Section 3.2.

We have also analyzed the importance of the time of initiation of treatment (t_0) on the course of the infection when using highly effective drugs. Fig. 8 shows the concentrations of infected (panel (a)) and healthy cells (panel(b)) as a function of time. In each panel, different plots correspond to different times chosen for the initiation of treatment ($t_0 = 50$, 150, 250 and 350 weeks, respectively). Note that the earlier treatment begins, the lower (higher) is the steady state concentration of infected (healthy) cells. Similar results (not shown) are obtained when low and moderate effectiveness is considered. The error bars shown in the graphs were obtained averaging over 50 samples and reflect the variations on the concentrations of infected and healthy cell behaviors among different patients that started the combined drug therapy at the same t_0. According to our results, the sooner the treatment begins, the greater would be the recovery of the healthy cell population driving the system away from the threshold of AIDS.

The graphs shown in the two previous figures illustrate the time evolution of the average cell concentration on the course of the infection, focusing on its steady state values with respect to the strength of effectiveness and the instant of initiation of treatment. However, it is also important to observe each sample behavior individually by analyzing the dependence of the results with respect to the concentration of infected or healthy cell baselines at the moment of the treatment's initiation. Such analysis leads to the estimate of the best time to start antiretroviral treatment during the course of HIV infection, an issue still controversial in HIV-infected patient care [57,58].

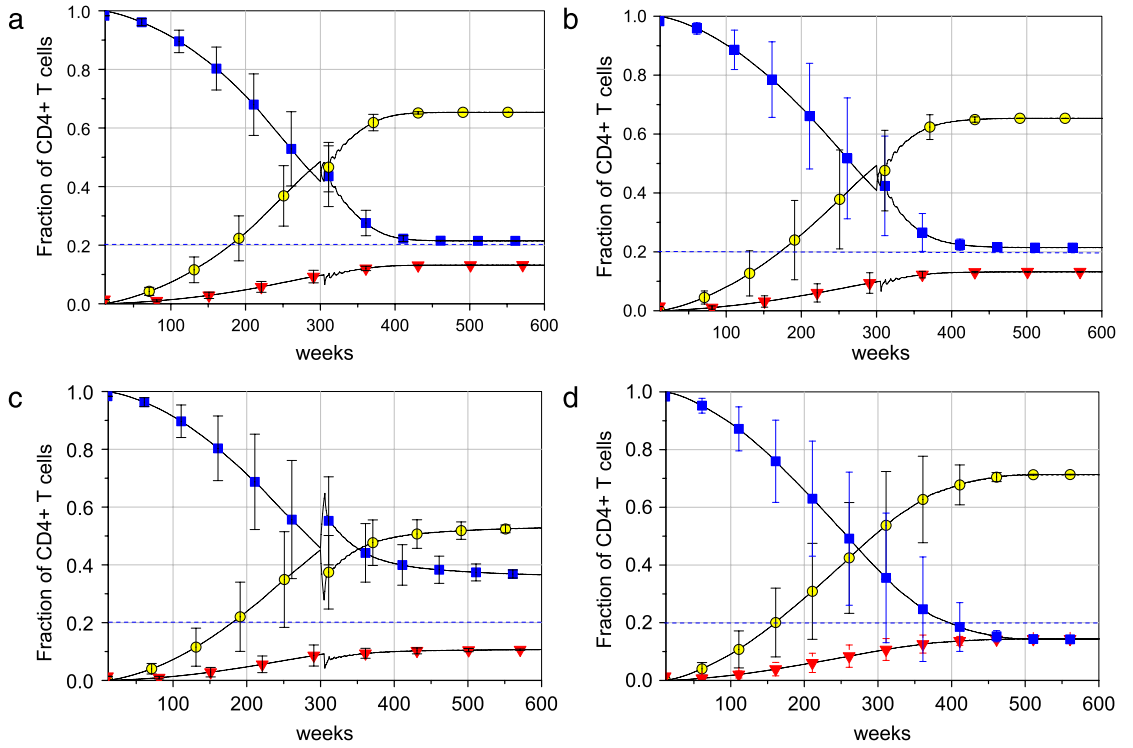

Fig. 6. Plots of the fractions of healthy (blue squares), infected A_1 plus A_2 (yellow circles) and dead (red down-triangles) cells for ARV treatments using low effectiveness ($p_{0j} = 0.5$) initiated at $t_0 = 300$ weeks. (a) RTI mono-therapy, (b) PI mono-therapy, (c) combined drug therapy (cART) and (d) absence of therapy. In all panels dashed blue lines mark the threshold of AIDS.

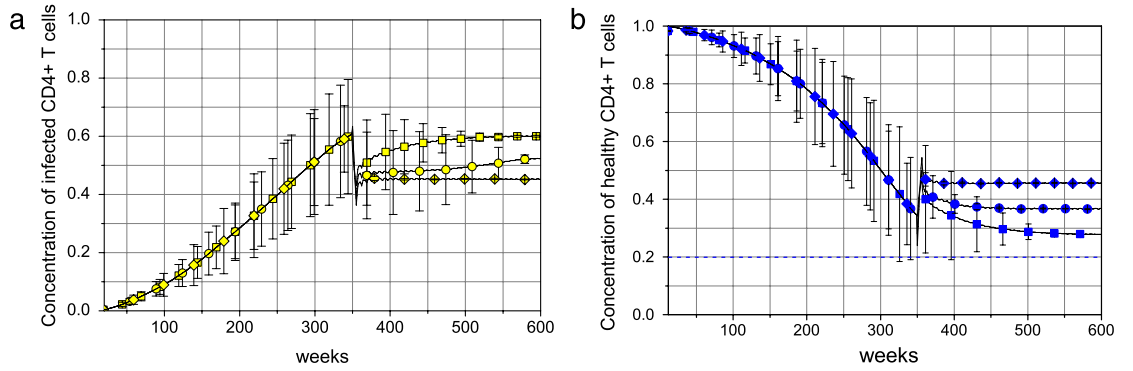

Fig. 7. Plots of the concentration of infected ($A_1 + A_2$) cells (panel (a)) and of the concentration of healthy cells (panel (b)) for a combined drug therapy of *low* ($p_{0\mathrm{RTI}} = p_{0\mathrm{PI}} = 0.5$, squares), *moderate* ($p_{0\mathrm{RTI}} = p_{0\mathrm{PI}} = 0.7$, circles) and *high* effectiveness ($p_{0\mathrm{RTI}} = p_{0\mathrm{PI}} = 0.9$, diamond) therapies initiated at $t_0 = 350$ weeks. In panel (b) the dashed blue line marks the threshold for AIDS.

Fig. 9 shows the density plot of the steady state concentration of healthy cells as a function of the effectiveness (p_{0j}) and the density of infected cells (D_{I0}) at the initiation of a cART. In this diagram three regions emerge depending on the course of infection after the treatment's initiation. On the upper left corner, there is a small region associated with the possibility of remission, provided drugs with high effectiveness are used during early infection, when the density of infected cells or viral load is very low. The borderline of this region is defined by samples exhibiting stationary concentrations of the order of 1% for infected cells and almost 99% of healthy cells. This region corresponding to 1.5%–2% of the entire plot's area represents the fraction of patients that may go over remission, an aspect that depends on the sensitivity of tests detecting viral particles.

When the effectiveness of drugs are less than 40%, no matter how early the treatment starts, the results indicate that the patient would acquire immunodeficiency syndrome. However, if the drug effectiveness is higher than 40% the treatment will always be worth keeping the patient healthy cell concentration above the AIDS threshold. In this case, as supported by clinical data [59], the lower the concentration of cells infected at the beginning of treatment, the greater the concentration of healthy cells at the steady state, reducing the risk of the patient reaching the onset of AIDS [59].

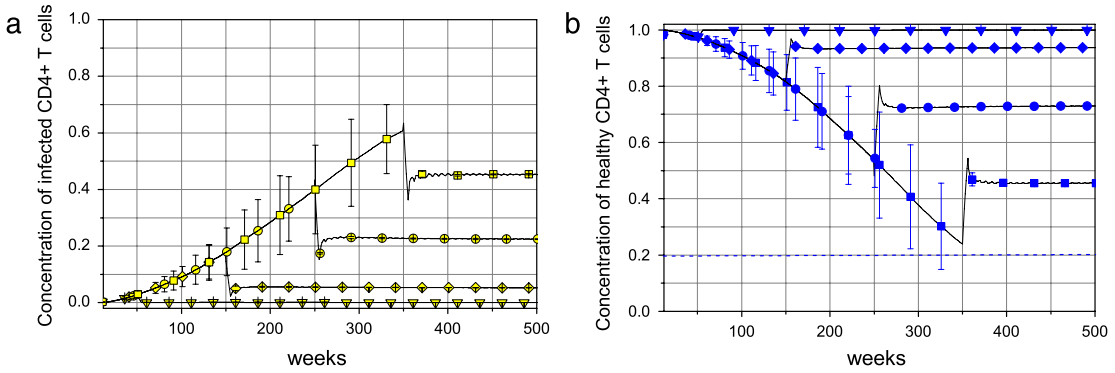

Fig. 8. Panel (a): plots of the concentration of infected A_1 plus A_2 for the combined RTI plus PI therapies of *high* effectiveness ($p_{01} = p_{02} = 0.9$) for therapies initiated at $t_0 = 50$ (down triangles), 150 (diamond), 250 (circles) and 350 (squares) weeks, after primary infection. Panel (b): corresponding graphs for the concentration of healthy cells. (For interpretation of the references to colour in this figure legend, the reader is referred to the web version of this article.)

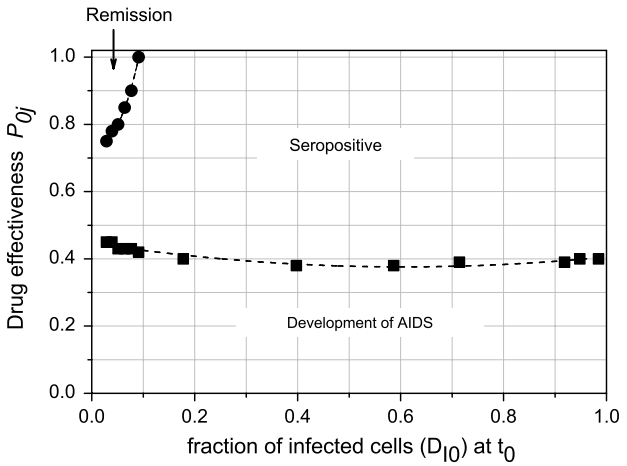

Fig. 9. Cell density diagram showing different behaviors of the dynamics of infection following cART therapy when varying the drug effectiveness p_{0j} and the initial fraction of infected cells D_{I0}. Solid circles delimitate the boundary of the remission region, while solid squares define the boundary of the AIDS region with the seropositive one. The remission region corresponds to samples that reach a steady-state with the concentration of infected cells below 0.01 corresponding to a viral load below the detection limit (50 viral copies/ml). The seropositive region corresponds to samples which end up with a finite concentration of infected cells but with healthy cell concentration still above the threshold to AIDS. The development of AIDS is the region of samples whose stationary value of infected cells is high and the healthy cell concentration is below the threshold to AIDS. Dashed lines are drawn from numerical fitting as a visual guide.

In Fig. 9, a rough estimate of the area of seropositive individuals indicates that it corresponds to 58%–59% of the total area leaving 38%–40% of it for the cases in which the healthy cell concentration is below the AIDS threshold and the individual becomes susceptible to opportunistic diseases.

Comparison with clinical data

In the 90's, several studies of the dynamics of treatment were conducted on the first and second years following the initiation of treatment [31,43]. In all cases, a significant increase in the concentration of the healthy cells during the first weeks of treatment when compared to its initial baseline (concentration of healthy cells at the beginning of the treatment) [60] was observed. All the studies have followed the same protocol performing periodic measurements of the $CD4^+$ T cell counts during the first two years after the treatment's initiation; the interval between any two counts varies among the different studies.

Some studies, whose data on the $CD4^+$ T cell counts are published, were chosen to be compared to the results obtained with the extended HIV-CA model introduced in this work. Figs. 10 and 11 compare the time evolution of the density of $CD4^+$ T cells obtained through the CA model with those measured on patients peripheral blood during clinical trials using mono-therapy and cART, respectively.

In Fig. 10, panel (a) shows the time-evolution of the average $CD4^+$ T cells counts, measured every three months in peripheral blood (per mm^3) of 28 patients submitted to mono-therapy over a period of 18 months as reported in Ref. [61].

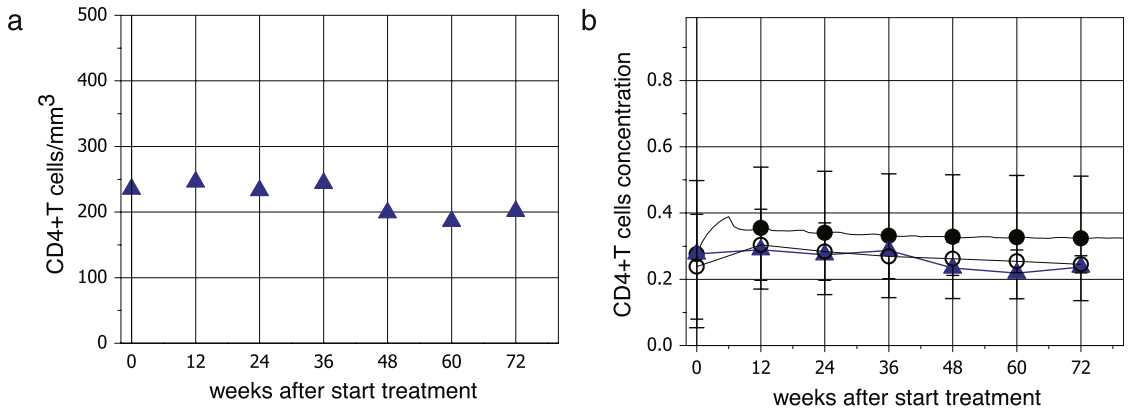

Fig. 10. Comparison with mono-therapy clinical data. Panel (a): plot of the time evolution of the average $CD4^+$ T cells counts in blood (per mm^3) of 28 patients reported in Ref. [61] (up triangles). Panel (b): plot of the time evolution of the average concentration of $CD4^+$ T cells obtained from 28 simulations with effectiveness $p_{0j} = 0.9$ (solid circles) and $p_{0j} = 0.5$ (open circles) and same plot of panel (a) but with values divided by the average cell $CD4^+$ T counts on non-infected individuals of 900 ± 200 cells μl (down triangles). The solid lines depict the results obtained from the models for every week. Error bars represent the standard deviation from simulation.

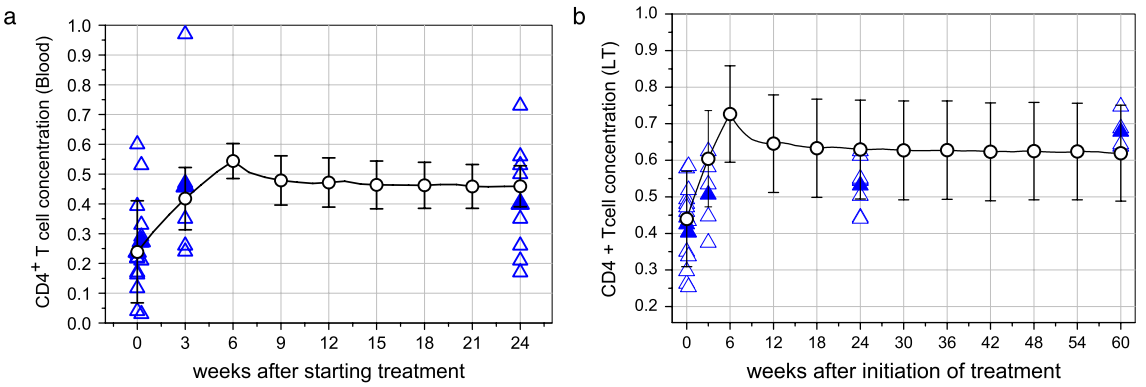

Fig. 11. Comparison with cART clinical data. Panel (a): time evolution of the fraction of healthy $CD4^+$ T cell counts in blood from nine patients collected at baseline, day 2 and weeks 3, and 24. Panel (b): similar plots for the fraction of healthy cells obtained from the lymphoid tissue (LT) at baseline, weeks 3, 24 and 60. In both panels open blue triangles represent the clinical data of each patient, solid blue triangles illustrate the corresponding average value and open circles indicate the plot emerging from the CA model for $p_{0j} = 0.9$ and 9 simulations. Clinical data are reported in Table 2 of Ref. [62]. The open circles depict the average values obtained for every week and the error bars represent the standard deviation obtained from model results.

Panel (b) shows the comparison of the clinical data and the ones obtained with the present model for mono-therapies with low and high drug effectiveness; in this case the concentrations are expressed in units of percentage relative to the average count of $CD4^+$ T cells for non-infected individuals. The theoretical results are generated by the CA model running a set of 28 simulations for which the beginning of the treatment is set for a concentration of $CD4^+$ T cells roughly equal to the value reported on the clinical data at initiation of therapy. The results obtained with our model reproduce the increase in $CD4^+$ T cell counts observed in the first weeks after the beginning of treatment and the subsequent gentle decline that occurs on the time scale of months as reported in Ref. [61]. It is interesting to note that the results that best reproduce the clinical data were obtained for drugs with low effectiveness ($p_{0j} = 0.5$).

In Ref. [62], the authors report the $CD4^+$ T cell counts in blood and lymphoid tissues of nine patients treated with cART during 60 weeks without any previous history of treatment. Fig. 11 shows the time course of the $CD4^+$ T cell counts for each patient (including its average values) in peripheral blood (a) and lymphoid tissues (b) compared to results (open circles) obtained by using the extended HIV-CA model. For the sake of clarity the clinical data is given in units of relative percentages to the average count of $CD4^+$ T cells in HIV seronegative individuals ($970 \pm 250/mm^3$ according to Ref. [62]). The results obtained with our model consider 90% of drug effectiveness and concentration of healthy cells at the beginning of the treatment around the same value of the initial baseline described in the clinical data. Despite the small amount of data and its large dispersion, our model captures the population growth of $CD4^+$ T cells observed in the first weeks after the treatment initiation and its smooth decrease in the scale of months that allow for the concentration of T cells remaining above the initial baseline.

Fig. 11(b) presents the $CD4^+$ T cell counts, measured in the lymphoid tissue (LT) (per μg) of the patients at initiation of the treatment (baseline) and at weeks 3, 24 and 60, as reported in Table 2 of Ref. [62]. This panel also displays the equivalent results obtained using the extended HIV-CA model considering treatments with 90% of drug effectiveness; the concentration of healthy cells at t_0 was chosen to be close to the value observed on the clinical data baselines. For an appropriated comparison the clinical data is shown in units of percentages relative to the average count of $CD4^+$ T cells in the lymphoid tissue of HIV of non-infected individuals ($320 \pm 39/\mu$g according to Table 1 of Ref. [62]). The results obtained including drug therapies to the HIV-CA model also reproduce the short timescale behavior observed in clinical data of $CD4^+$ T cell counts in lymphoid tissues, i.e. a rapid population growth in the first weeks. In the timescale of months, however, the model results indicate stabilization towards a steady state, while the clinical data reveal a smooth growth. The same timescales and behavior observed in Refs. [60,62] were also observed in many other clinical studies on the evolution of $CD4^+$ T and $CD8^+$ T cell counts (see for instance Fig. 2(B) and (C) of Ref. [63], Fig. 1(C) and (D) of Ref. [60], Fig. 1(B) and (C) of Ref. [64] and Fig. 7 of Ref. [21]).

Concerning the comparisons between the clinical data and model results, illustrated in Figs. 10 and 11, it is important to emphasize two points. First, the relevant result of this study concerns the reproduction of time scales in which significant changes in the $CD4^+$ T cell count take place during treatment of the infection. The comparison of the numeric values of the clinical data (fractions) with those obtained by the model at each time must be regarded in a qualitative manner, since to estimate the fractions of healthy or infected $CD4^+$ T cells in blood (per μL) or in LT (per μg) during the infection it is necessary to know such values in non-infected individuals, which vary appreciably from individual to individual according to several factors. Second, the only parameters used to describe the treatment in the model were the effectiveness of drugs (p_{0j}) and the time of the treatment initiation (t_0), which for the comparisons done were chosen in such a way that the density of healthy cells was close of the value of baseline clinical data. All other parameters of the model are chosen and fixed at the beginning of the course of infection, which is described by the HIV-CA model. We have also observed that when other p_{0j} values are considered, the time scales in the horizontal axis remain unchanged and only the values on the vertical axis of the graphs are changed.

In the next Section we will explore in more detail the model results in a short timescale when compared with data.

3.2. Dynamics of HIV infection under ARV therapy in short timescale after therapy

The dynamics of HIV infection in patients under cART over a short time scale has generally been investigated through measurements of the viral load in plasma. The quantitative relationship between the number of virus producing cells and plasma viral load is not well established but a non-linear relationship between viral load in plasma and HIV νRNA-expressing cells in lymph node tissues was observed in Ref. [65].

The concentration of HIV RNA declines rapidly in a few weeks after starting treatment, as reported on measurements in plasma [55,66,56] and in other fluids such as the cerebrospinal one [67,66], as well as in follicular dendritic and mononuclear cells of the lymphoid tissues [68]. The patterns of the dynamics of viral load have also been investigated with the aid of ordinary differential equation mathematical models [6,69–72,38]. Two dynamic phases can be separated from these observations and studies, apart from the initial pharmacological delay of the order of hours after initiation of therapy. In the first phase, there is an exponential decay in 2–4 decades of magnitude (in $\log_{10}$ scale) on a timescale of 4–12 weeks, which is followed by a second phase of slower decay in time scale of the order of months. The reduction of virus load in the first phase is attributed to the clearance of free virus particles by ARV drugs and the consequent decline in productively infected cells. The attenuation of this decay is attributed to the combined effect of the emergence of resistant virus [8,40], the imperfect effectiveness of drugs ($<100\%$) and the existence of reservoirs of latently infected cells, such as resting memory $CD4^+$ T cells or dendritic cells and macrophages present in the lymph nodes, which may continuously produce virus particles [3,68,70,71,73].

To validate the present CA model, a comparison was made between clinical data of HIV RNA count of individuals under cART with results for infected cells. The time scales of HIV RNA count in plasma are comparable to those seen in infected follicular dendritic and mononuclear cells of the lymphoid tissues [68].

Fig. 12 displays the early stages trajectories of HIV RNA counts (in $\log_{10}$ (RNA) copies/mL) for 42 patients enrolled in the AIDS Clinical Trial Study-A5055 [55]. Panel (a) illustrates the profiles of the viral load observed in the first 35 days after initiation of treatment, while panel (b) extends the observations from day zero up to 200 days. Two time scales are evident from these data. A short-term one of about 35 days during a rapid decrease in HIV RNA count of approximately two to three orders of magnitude and a long time scale (of the order of months) with a slower decay of about one order of magnitude. Similar time scales can also be seen in other clinical data after the initiation of antiretroviral therapies and have been investigated by several authors, e.g. Refs. [53,69–74].

The effects of therapy over short time scales can be observed by analyzing the concentrations of infected cells in the framework of the model presented here, when focusing on its evolution just after the initiation of the treatment t_0. For the sake of comparison, Fig. 13 illustrates the course of the infected $CD4^+$ T cells for 42 independent runs (same parameters and different initial configurations) during 5 weeks (panel a) and 20 weeks (panel b), after initiation of treatment at $t_0 = 300$ weeks. The results show that the concentration of infected cells in most of the cases declines rapidly, reaching a minimum value 5 weeks after initiation of drug therapy. The same characteristic timescale is observed in the clinical data shown in Fig. 13.

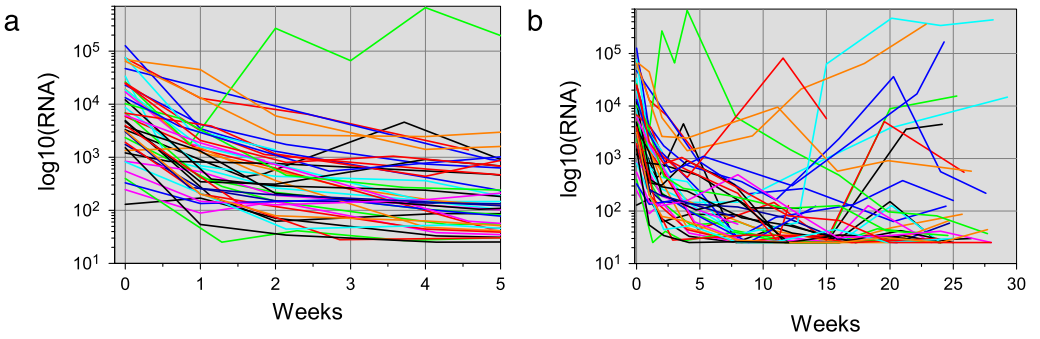

Fig. 12. Course of the concentration of plasma HIV-1 RNA (viral load) from a group of 42 subjects enrolled in the AIDS Clinical Trial Study [55]. Panel (a) Interval of the first 5 weeks (b) Interval for the 28 weeks of study. Colors were used to differentiate between each individual. (For interpretation of the references to colour in this figure legend, the reader is referred to the web version of this article.)

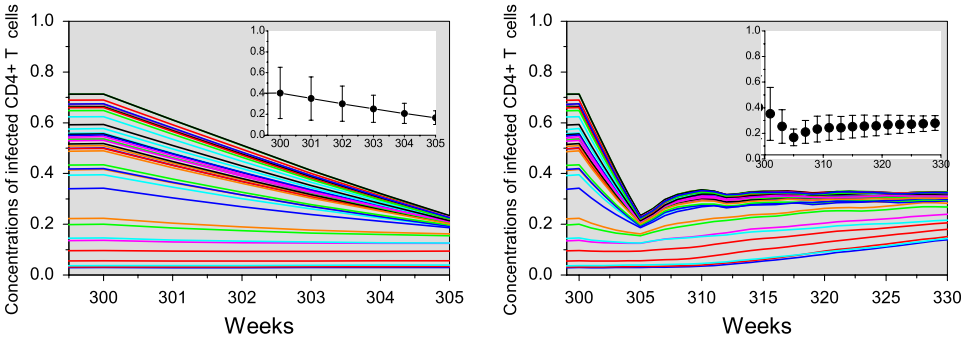

Fig. 13. Plots of the concentration of infected $CD4^+$ T cells after beginning of therapy for 42 independent simulations, considering effectiveness parameter $p_{01} = p_{02} = 0.7$ and the treatment initiating at $t_0 = 300$ weeks. Panel (a) Interval of the first 5 weeks afterwards; (b) Interval of 30 weeks afterwards. The insets display the plot for the average concentrations with error bars indicated. Initial parameters: $p_{\text{HIV}} = 0.05$, $p_{\text{infec}} = 0.00001$, $p_{\text{reg}} = 0.99$ and $\tau = 4$. (For interpretation of the references to colour in this figure legend, the reader is referred to the web version of this article.)

The comparisons exhibited in Figs. 12 and 13 show that our model reproduces the timescales and behavior of $CD4^+$ T cell counts observed during the first weeks after the initiation of cART as observed on clinical data, therefore validating the model to describe the follow up of (mono or combined) drug therapies after its initiation.

4. Conclusions

In this work the dynamics of HIV infection under the action of antiretroviral therapy is investigated using a cellular automata model. The course of the infection before the beginning of treatment ($t = t_0$) is described by the HIV-CA model previously proposed in Ref. [17]. To account for the mechanisms of the treatment at $t > t_0$, three new states were incorporated to the $CD4^+$ T healthy-cell automata with their respective dynamic rules describing the process of absorption of the antiretroviral drugs. The efficacy of the treatment is taken into account through a self-adjusting process for the effectiveness of each type of drug according to the viral load (infected cell counts) at each time step. This mechanism is the key point of the present model.

The mechanism of self-adjusting the drug's effectiveness allows us to describe separately the ARV treatment of each individual, since the efficacy of each drug is fixed by the particular value of the fraction of infected cells at each time instant of the simulation. Moreover, this mechanism also incorporates the hypothesis of the high mutation rate of HIV as responsible for the loss of drug efficacy over time. These features are in accordance with the great variability observed in the patients' clinical data in both the short time scale after initiation of treatment, as well as throughout the subsequent course of infection.

The long-term results emerging from the CA model suggest that the combination of antiretroviral treatments conducted with *highly* potent drugs and starting when the population of infected cells is low, can lead to a course of the infection characterized by a stable population of infected cells below detectable levels. If the drugs have *moderate* effectiveness, however, the behavior may be stable with low levels of infected cells corresponding to that of healthy $CD4^+$ T cells at levels above the threshold for the development of AIDS. For *low* drug effectiveness the T cell counts may remain below the threshold. When compared to clinical data the present model reproduces the qualitative behavior observed in the evolution of the population of $CD4^+$ T cells during a period of 18 months, but the best results are obtained for ineffective drugs ($p_{0j} = 0.5$).

When analyzed on a short time scale after initiation of treatment, the results obtained by the simulations show clearly that in most cases there is a marked decrease of the population of infected cells in the range of about 5 weeks, as observed

in most of the equivalent cases reported in the literature. The occurrence of this sharp drop in viral load at a short time scale of the order of weeks after initiation of treatment was seen in the clinical count of HIV-1 RNA in plasma, as illustrated in Figs. 12 and 13 of this study. Furthermore, following the sharp reduction in viral load, the results also show a subsequent rebound in the concentration of infected cells. Such rebound behavior was also observed in some measurements of HIV-1 RNA in plasma, which may be associated with resistance to cART as discussed in Ref. [72].

As a general conclusion of this study, we found that the HIV-CA original model [17] with the inclusion of mechanisms that describe the processes of antiretroviral therapies, based on a biological hypothesis, is capable of reproducing the time scales of the inherent phenomena of the dynamics of HIV infection in patients under drug therapies.

As concluding remarks, we emphasize that the results that emerge from the simulations show a large dispersion with respect to the initial concentration of infected cells at $t = 0$, the initial contamination characteristic of each patient, while the other parameters are kept constant. Such variability remains after the beginning to treatment at $t = t_0$ in accordance with the observed clinical data. In addition, we expect that the proposed model can be used in future as a tool to investigate different treatment protocols. The starting time t_0, the period of application of drugs, the effectiveness parameter of each drug p_{0j} can be varied in a simple way to describe other aspects of the HIV infection such as pharmacokinetic effects of adherence and to establish more effective treatment strategies.

References

[1] World Health Organization, Global HIV/AIDS response, Technical Report, World Health Organization, 2011.
[2] Didier Trono, Carine Van Lint, Christine Rouzioux, Eric Verdin, Francoise Barré-Sinoussi, Tae-Wook Chun, Nicolas Chomont, HIV persistence and the prospect of long-term drug-free remissions for HIV-infected individuals, Science 329 (5988) (2010) 174–180.
[3] Valentin Le Douce, Georges Herbein, Olivier Rohr, Christian Schwartz, Molecular mechanisms of HIV-1 persistence in the monocyte-macrophage lineage, Retrovirology 7 (2010) 32.
[4] Douglas D. Richman, David M. Margolis, Martin Delaney, Warner C. Greene, Daria Hazuda, Roger J. Pomerantz, The challenge of finding a cure for HIV infection, Science 323 (5919) (2009) 1304–1307.
[5] Alan S. Perelson, Denise E. Kirschner, Rob De Boer, Dynamics of HIV infection of CD4$^+$T cells, Mathematical Biosciences 114 (1) (1993) 81–125.
[6] Alan S. Perelson, Avidan U. Neumann, Martin Markowitz, John M. Leonard, David D. Ho, HIV-1 dynamics in vivo: virion clearance rate, infected cell life-span, and viral generation time, Science 271 (5255) (1996) 1582–1586.
[7] Denise Kirschner, G.F. Weeb, Understanding drug resistance for monotherapy treatment of HIV infection, Bulletin of Mathematical Biology 59 (4) (1997) 763–785.
[8] Xiping Wei, Sajal K. Ghosh, Maria E. Taylor, Victoria A. Johnson, Emilio A. Emini, Paul Deutsch, Jeffrey D. Lifsonparallel, Sebastian Bonhoeffer, Martin A. Nowak, Beatrice H. Hahn, Michael S. Saag, George M. Shaw, Viral dynamics in human immunodeficiency virus type 1 infection, Nature 373 (1995) 117–122.
[9] Martin A. Nowak, Robert M. May, Virus Dynamics—Mathematical Principles of Immunology and Virology, Oxford University Press, 2000.
[10] Alan S. Perelson, Patrick W. Nelson, Mathematical analysis of HIV-1 dynamics in vivo, SIAM Review 41 (1) (1999) 3–44.
[11] Alberto Landi, Alberto Mazzoldi, Chiara Andreoni, Matteo Bianchi, Andrea Cavallini, Marco Laurino, Leonardo Ricotti, Rodolfo Iuliano, Barbara Matteoli, Luca Ceccherini-Nelli, Modelling and control of HIV dynamics, Computer Methods and Programs in Biomedicine 89 (2007).
[12] Libin Rong, Alan S. Perelson, Modeling HIV persistence, the latent reservoir, and viral blips, Journal of Theoretical Biology 260 (2) (2009) 308–331.
[13] Freda Wasserstein-Robbins, A mathematical model of HIV infection: simulating T4, T8, macrophages, antibody, and virus via specific anti-HIV response in the presence of adaptation and tropism, Bulletin of Mathematical Biology (2010) 1208–1253.
[14] R.J. Smith, L.M. Wahl, Distinct effects of protease and reverse transcriptase inhibition in an immunological model of HIV-1 infection with impulsive drug effects, Bulletin of Mathematical Biology 66 (5) (2004) 1259–1283.
[15] O. Krakovska, L.M. Wahl, Optimal drug treatment regimens for HIV depend on adherence, Journal of Theoretical Biology 246 (3) (2007) 499–509.
[16] Jorge Ferreira, Esteban A. Hernandez-Vargas, Richard H. Middleton, Computer simulation of structured treatment interruption for HIV infection, Computer Methods and Programs in Biomedicine 104 (2) (2011) 50–61.
[17] Rita Maria Zorzenon dos Santos, Sérgio Coutinho, Dynamics of HIV infection: a cellular automata approach, Physical Review Letters 87 (16) (2001) 168102.
[18] Ch.F. Kougias, J. Schulte, Simulating the immune response to the HIV-1 virus with cellular automata, Journal of Statistical Physics 60 (1990) 263–273. http://dx.doi.org/10.1007/BF01013677.
[19] R.B. Pandey, D. Stauffer, Metastability with probabilistic cellular automata in an HIV infection, Journal of Statistical Physics 61 (1–2) (1990) 235–240.
[20] R.B. Pandey, Cellular automata approach to interacting cellular network models for the dynamics of cell population in an early HIV infection, Physica A: Statistical Mechanics and its Applications 179 (3) (1991) 442–470.
[21] A.T. Haase, Population biology of HVI-1 infection: viral and CD4$^+$ T cell demographics and dynamics in lymphatic tissues, Annual Review of Immunology 17 (1999) 625–656.
[22] P.H. Figueirêdo, S. Coutinho, R.M. Zorzenon dos Santos, Robustness of a cellular automata model for the HIV infection, Physica A: Statistical Mechanics and its Applications 387 (26) (2008) 6545–6552.
[23] Guillermo Solovey, Fernando Peruani, Silvina Ponce Dawson, Rita Maria Zorzenon dos Santos, On cell resistance and immune response time lag in a model for the HIV infection, Physica A: Statistical Mechanics and its Applications 343 (2004) 543–556.
[24] Matthew C. Strain, Herbert Levine, Comment on "dynamics of HIV infection: a cellular automata approach", Physical Review Letters 89 (2002) 219805.
[25] E. Burkhead, J. Hawkins, D. Molinek, A dynamical study of a cellular automata model of the spread of HIV in a lymph node, Bulletin of Mathematical Biology 71 (1) (2009) 25–74.
[26] Peter M.A. Sloot, Fan Chen, Charles Boucher, Cellular automata model of drug therapy for HIV infection, in: ACRI'01: Proceedings of the 5th International Conference on Cellular Automata for Research and Industry, Springer-Verlag, London, UK, 2002, pp. 282–293.
[27] A. Benyoussef, N.E. HafdiAllah, A. ElKenz, H. Ez-Zahraouy, M. Loulidi, Dynamics of HIV infection on 2D cellular automata, Physica A 322 (2003) 506–520.
[28] M.A. Peer, N.A. Shan, K.A. Khan, Cellular automata and its advances to drug therapy for HIV infection, Indian Journal of Experimental Biology 42 (2) (2004) 131–137.
[29] Veronica Shi, Abdessamad Tridane, Yang Kuang, A viral load-based cellular automata approach to modeling HIV dynamics and drug treatment, Journal of Theoretical Biology 253 (1) (2008) 24–35.
[30] Monamorn Precharattana, Arthorn Nokkeaw, Wannapong Triampo, Darapond Triampo, Yongwimon Lenbury, Stochastic cellular automata model and Monte Carlo simulations of CD4$^+$T cell dynamics with a proposed alternative leukapheresis treatment for HIV/AIDS, Computers in Biology and Medicine 41 (7) (2011) 546–558.
[31] Lucia Palmisano, Stefano Vella, A brief history of antiretroviral therapy of HIV infection: success and challenges, Annali dell'Istituto Superiore di Sanità 47 (1) (2011) 44–48.
[32] Kosuke Miyauchi, Yuri Kim, Olga Latinovic, Vladimir Morozov, Gregory B. Melikyan, HIV enters cells via endocytosis and dynamin-dependent fusion with endosomes, Cell 137 (3) (2009) 433–444.

[33] Warner C. Greene, B. Matija Peterlin, Charting HIV's remarkable voyage through the cell: basic science as a passport to future therapy, Nature Medicine 8 (7) (2001) 673–680. 07.
[34] B.Matija Peterlin, Didier Trono, Hide, shield and strike back: how HIV-infected cells avoid immune eradication, Nature Reviews Immunology 3 (2) (2003) 97–107.
[35] G. Pantaleo, C. Graziozi, A.S. Fauci, The immunopathogenesis of immunodeficiency virus infection, New England Journal of Medicine 238 (1993) 327.
[36] J.M. Coffin, HIV population dynamics in vivo: implications for genetic variation, pathogenesis, and therapy, Science (New York, NY) 267 (5197) (1995) 483–489.
[37] Eric S. Daar, Tarsem Moudgil, Richard D. Meyer, David D. Ho, Transient high levels of viremia in patients with primary human immunodeficiency virus type 1 infection, New England Journal of Medicine 324 (14) (1991) 961–964. 01.
[38] Alan S. Perelson, Modelling viral and immune system dynamics, Nature Reviews Immunology 2 (1) (2002) 28–36.
[39] Anthony S. Fauci, HIV and AIDS: 20 years of science, Nature Medicine 9 (7) (2003) 839–843.
[40] David D. Ho, Avidan U. Neumann, Alan S. Perelson, Wen Chen, John M. Leonard, Martin Markowitz, Rapid turnover of plasma virions and CD4 lymphocytes in HIV-1 infection, Nature 373 (1995) 123–126.
[41] Alon Herschhorn, Amnon Hizi, Retroviral reverse transcriptases, Cellular and Molecular Life Sciences 67 (16) (2010) 2717–2747.
[42] Yazan El Safadi, Valérie Vivet-Boudou, Roland Marquet, HIV-1 reverse transcriptase inhibitors, Applied Microbiology and Biotechnology 75 (4) (2007) 723–737.
[43] Carlo Federico Perno, The discovery and development of HIV therapy: the new challenges, Annali dell'Istituto Superiore di Sanitá 4 (1) (2011) 41–43.
[44] Michael F. Schneider, Stephen J. Gange, Carolyn M. Williams, Kathryn Anastos, Ruth M. Greenblatt, Lawrence Kingsley, Roger Detels, Alvaro Muñoz, Patterns of the hazard of death after AIDS through the evolution of antiretroviral therapy: 1984–2004, AIDS 19 (17) (2005) 2009–2018.
[45] Christophe Marchand, Kasthuraiah Maddali, Mathieu Métifiot, Yves Pommier, HIV-1 IN inhibitors: 2010 update and perspectives, Current Topics in Medicinal Chemistry 9 (11) (2009) 1016–1037.
[46] Annemarie M.J. Wensing, Noortje M. van Maarseveen, Monique Nijhuis, Fifteen years of HIV protease inhibitors: raising the barrier to resistance, Antiviral Research 85 (1) (2010) 59–74.
[47] David D. Ho, Dynamics of HIV-1 replication in vivo, Journal of Clinical Investigation 99 (1997) 2565–2567.
[48] M.A. Nowak, Roy M. Anderson, Maarten V. Boerlijts, S. Bonhoeffer, Robert M. May, HIV-1 evolution and disease progression, Science 274 (1996) 1008–1011.
[49] Tae-wook Chun, Lucy Carruth, Diana Finzi, Xuefei Shen, Joseph A. DiGiuseppe, Harry Taylor, Monika Hermankova, Karen Chadwick, Joseph Margolik, Thomas C. Quinn, Yen-Hong Kuo, Ronald Brookmeyer, Martha A. Zeiger, Patricia Barditch-Crovo, Robert F. Siliciano, Quantification of latent tissue reservoirs and total body viral load in HIV-1 infection, Nature 387 (1997) 182–188.
[50] Tae-Wook Chun, Anthony S. Fauci, Latent reservoirs of HIV: obstacles to the eradication of virus, Proceedings of the National Academy of Sciences of the United States of America 96 (20) (1999) 10958–10961.
[51] Janet D. Siliciano, Joleen Kajdas, Diana Finzi, Thomas C. Quinn, Karen Chadwick, Joseph B. Margolick, Colin Kovacs, Stephen J. Gange, Robert F. Siliciano, Long-term follow-up studies confirm the stability of the latent reservoir for HIV-1 in resting $CD4^+$T cells, Nature Medicine 9 (6) (2003) 727–728.
[52] Tae-Wook Chun, David C. Nickle, J. Shawn Justement, Danielle Large, Alice Semerjian, Marcel E. Curlin, M. Angeline O'Shea, Claire W. Hallahan, Marybeth Daucher, Douglas J. Ward, Susan Moir, James I. Mullins, Colin Kovacs, Anthony S. Fauci, HIV-infected individuals receiving effective antiviral therapy for extended periods of time continually replenish their viral reservoirs, Journal of Clinical Investigation 115 (11) (2005) 3250–3255.
[53] Yangxin Huang, Tao Lu, Modeling long-term longitudinal HIV dynamics with application to an AIDS clinical study, The Annals of Applied Statistics 2 (4) (2008) 1384–1408.
[54] David R. Bangsberg, Edwin D. Charlebois, Robert M. Grant, Mark Holodniy, Steven G. Deeks, Sharon Perry, Kathleen Nugent Conroy, Richard Clark, David Guzman, Andrew Zolopa, Andrew Moss, High levels of adherence do not prevent accumulation of HIV drug resistance mutations, AIDS 17 (13) (2003) 1925–1932.
[55] Edward P. Acosta, Hulin Wu, Scott M. Hammer, Song Yu, Daniel R. Kuritzkes, Ann Walawander, Joseph J. Eron, Carl J. Fichtenbaum, Carla Pettinelli, Denise Neath, Elaine Ferguson, Alfred J. Saah, John G. Gerber, Comparison of two indinavir/ritonavir regimens in the treatment of HIV-infected individuals, Journal of Acquired Immune Deficiency Syndromes 37 (3) (2004) 1358–1366.
[56] Vladimir Novitsky, Rui Wang, Hermann Bussmann, Shahin Lockman, Marianna Baum, Roger Shapiro, Ibou Thior, Carolyn Wester, C. William Wester, Anthony Ogwu, Aida Asmelash, Rosemary Musonda, Adriana Campa, Sikhulile Moyo, Erik van Widenfelt, Madisa Mine, Claire Moffat, Mompati Mmalane, Joseph Makhema, Richard Marlink, Peter Gilbert, George R. Seage, Victor DeGruttola, M. Essex, HIV-1 subtype C-infected individuals maintaining high viral load as potential targets for the "test-and-treat" approach to reduce HIV transmission, PLoS One 5 (4) (2010) e10148.
[57] When To Start Consortium, Timing of initiation of antiretroviral therapy in AIDS-free HIV-1-infected patients: a collaborative analysis of 18 HIV cohort studies, Lancet 373 (9672) (2009) 1352–1363.
[58] N. Siegfried, O.A. Uthman, G.W. Rutherford, Optimal time for initiation of antiretroviral therapy in asymptomatic, HIV-infected, treatment-naive adults, Cochrane Database of Systematic Reviews 17 (3) (2010) CD008272.
[59] The Opportunistic, Infections Project, and Observational HIV, CD4 cell count and the risk of AIDS or death in HIV-infected adults on combination antiretroviral therapy with a suppressed viral load: a longitudinal cohort study from COHERE, PLoS Medicine 9 (3) (2012) e1001194.
[60] B. Autran, G. Carcelain, T.S. Li, C. Blanc, D. Mathez, R. Tubiana, C. Katlama, P. Debré, J. Leibowitch, Positive effects of combined antiretroviral therapy on $CD4^+$T cell homeostasis and function in advanced HIV disease, Science 277 (5322) (1997) 112–116.
[61] A. Ruffault, C. Michelet, C. Jacquelinet, O. Guist'au, N. Genetet, C. Bariou, R. Colimon, F. Cartier, The prognostic value of plasma viremia in HIV-infected patients under AZT treatment: a two-year follow-up study, Journal of Acquired Immune Deficiency Syndromes and Human Retrovirology 9 (4) (1995) 243–248.
[62] Zhi-Qiang Zhang, Daan W. Notermans, Gerald Sedgewick, Winstor Cavert, Stephen Wietgrefe, Mary Zupancic, Kristin Gebhard, Keith Henry, Lawrence Boies, Zongming Chen, Marc Jenkins, Roger Mills, Hugh McDade, Carolyn Goodwin, Caspar M. Schuwirth, Sven A. Danner, Ashley T. Haase, Kinetics of $CD4^+$T cell repopulation of lymphoid tissues after treatment of HIV-1 infection, PNAS 95 (3) (1998) 1154–1159.
[63] Ferdinand W.N.M. Wit, Remko van Leeuvwen, Gerrit Jan Weverling, Suzanne Jurriaans, Klaas Nauta, Radjin Steingrover, Johan Schuijtemaker, Xander Eyssen, David Fortuin, Marjan Weeda, Frank de Wolf, Peter Reiss, Sven A. Danner, Joep M.A. Lange, Outcome and predictors of failure of higlhy active antiretroviral therapy: one-year follow-up of a cohort of human immunodeficiency virus type 1-infected persons, The Journal of Infectious Diseases 179 (1999) 790–798.
[64] Gilbert R. Kaufmann, Luc Perrin, Guiseppe Pantaleo, Milos Opravil, Hansjakob Furrer, Amalio Telenti, Bernard Hirschel, Bruno Ledergerber, Pietro Vernazza, Enos Bernasconi, Martin Rickenbach, Matthias Egger, Manuel Battegay, CD4 T-lymphocyte recovery in individuals with advanced HIV-1 infection receiving potent antiretroviral therapy for 4 years: the Swiss HIV cohort study, Archives of Internal Medicine 163 (18) (2003) 2187–2195.
[65] R.D. Hockett, J.M. Kilby, C.A. Derdeyn, M.S. Saag, M. Sillers, K. Squires, S. Chiz, M.a. Nowak, G.M. Shaw, R.P. Bucy, Constant mean viral copy number per infected cell in tissues regardless of high, low, or undetectable plasma HIV RNA, The Journal of Experimental Medicine 189 (10) (1999) 1545–1554.
[66] R.H. Enting, J.M. Prins, S. Jurriaans, K. Brinkman, P. Portegies, J.M. Lange, Concentrations of human immunodeficiency virus type 1 (HIV-1) RNA in cerebrospinal fluid after antiretroviral treatment initiated during primary HIV-1 infection, Clinical Infectious Diseases 32 (7) (2001) 1095–1099.
[67] Asa Mellgren, Andrea Antinori, Paola Cinque, Richard W. Price, Christian Eggers, Lars Hagberg, Magnus Gisslén, Cerebrospinal fluid HIV-1 infection usually responds well to antiretroviral treatment, Antiviral Therapy 10 (6) (2005) 701–707.
[68] W. Cavert, Kinetics of response in lymphoid tissues to antiretroviral therapy of HIV-1 infection, Science 276 (5314) (1997) 960–964.
[69] H. Wu, A.A. Ding, Population HIV-1 dynamics in vivo: applicable models and inferential tools for virological data from AIDS clinical trials, Biometrics 55 (2) (1999) 410–418.
[70] A.V.M. Herz, S. Bonhoeffer, R.M. Anderson, R.M. May, M.A. Nowak, Viral dynamics in vivo: limitations on estimates of intracellular delay and virus decay, Proceedings of the National Academy of Sciences of the United States of America 93 (14) (1996) 7247–7251.

[71] Alan S. Perelson, Paulina Essunger, Yunzhen Cao, Mika Vesanen, Arlene Hurley, Kalle Saksela, Martin Markowitz, David Ho, Decay characteristics of HIV-1-infected compartments during combination therapy, Nature 387 (6629) (1997) 188–191.
[72] Anthony P. Fitzgerald, Victor G. DeGruttola, Florin Vaida, Modelling HIV viral rebound using non-linear mixed effects models, Statistics in Medicine 21 (14) (2002) 2093–2108.
[73] Viktor Müller, Javier Flavio Vigueras-Gómez, Sebastian Bonhoeffer, Decelerating decay of latently infected cells during prolonged therapy for human immunodeficiency virus type 1 infection, Journal of Virology 76 (17) (2002) 8963–8965.
[74] Viviana Simon, David D. Ho, HIV-1 dynamics *in vivo: implications for therapy*, Nature Reviews Microbiology 1 (2003) 181–190.